CONDENSED MATTER PHYSICS

Making a case for femto-phono-magnetism with FePt

Sangeeta Sharma[1]*, Sam Shallcross[1], Peter Elliott[1], J. Kay Dewhurst[2]

In the field of femtomagnetism, magnetic matter is controlled by ultrafast laser pulses; here, we show that coupling phonon excitations of the nuclei to spin and charge leads to femto-phono-magnetism, a powerful route to control magnetic order at ultrafast times. With state-of-the-art theoretical simulations of coupled spin, charge, and lattice dynamics, we identify strong nonadiabatic spin-phonon coupled modes that dominate early time spin dynamics. Activating these phonon modes that we show leads to an additional (up to 40% extra) loss of moment in iron-platinum occurring within 40 femtoseconds of the pump laser pulse. Underpinning this enhanced ultrafast loss of spin moment, we identify a physical mechanism in which minority spin current drives an enhanced intersite minority charge transfer, in turn promoting increased on-site spin flips. Our finding demonstrates that the nuclear system, often assumed to play the role of an energy and angular momentum sink, when selectively preexcited, can play a profound role in controlling femtosecond spin dynamics in materials.

INTRODUCTION

The speed at which information is stored and processed is determined by the fundamental time scales at which matter can be manipulated by external fields (*1*). The fastest such control is through the interaction of matter with the electromagnetic field of light, with ultrafast laser control over magnetic order now well established as a key low-energy route to controlling microscopic order (*2*). To leading order, however, the electromagnetic field does not couple directly to spin (*3*), and so, control over magnetic order proceeds indirectly through charge excitations.

At femtosecond time scales, this can occur either through spin transfer between magnetic sublattices (*4*, *5*), through manipulation of spin-orbit coupling (*6*–*8*) and spin-orbit torques (*9*), or at later time scales via the exchange interaction (*10*). In all these processes, the lattice plays the vital role of an energy and momentum reservoir into which the angular momentum lost due to demagnetization is transferred (*11*). Insight into process was recently vividly provided through an experiment in which femtosecond scale creation of polarized (i.e., circular) phonons was demonstrated (*12*).

The importance of the lattice in demagnetization suggests that it may provide a route to directly control spin dynamics via excitation before the laser pulse that induces the spin dynamics. Recently, the lattice has been used as a route to directly control matter through the excitation of infrared (IR) phonon modes (*13*–*19*). However, the idea of phonomagnetism (*20*, *21*), i.e., manipulation of spins via nuclear dynamics, only now is beginning to be examined as an additional degree of freedom via which spin can be dynamically manipulated. The role that selective coherent excitation of the lattice can play in the manipulation of magnetic matter at the fastest possible time scales, i.e., femto-phono-magnetism, remains unexplored, and this is the central question that we will address in this work.

As far as theoretical treatment of light-matter interaction is concerned, time-dependent density functional theory (TDDFT) (*22*) is a fully quantum mechanical and ab initio method that has been shown to be very successful not only in providing insight into experiments but also in predicting new phenomena (*4*, *5*, *23*, *24*). In the present work, we provide a method, suitable for extended solids, via which charge and spin dynamics within TDDFT can be coupled to the motion of the nuclei. Using this technique and with the example of FePt, we address the question of what role lattice phonon excitations play in the dynamics of magnetic order on ultrafast time scales. The choice of FePt for our study is based on a number of factors: (i) As a multicomponent magnet with strong spin-orbit coupling, the spin dynamics are especially rich, e.g.,, the material exhibits the optical intersite spin transfer (OISTR) effect (*4*); (ii) it furthermore has strong spin-phonon coupling (*25*), making it a likely candidate for phonomagnetism; and (iii) the material is technologically important for ultradense magnetic recording (*26*–*28*) and, moreover, has recently has shown to exhibit all optical magnetization reversal (*29*), and these switching times would reduce with faster phonon-induced early time demagnetization. Our key finding from this study is that selective lattice excitation before the laser pulse can result in substantially enhanced demagnetization, behavior in notable contrast to the commonly held view that the lattice acts as a reservoir for momentum at early times and aids remagnetization at longer time scales. Furthermore, we find that these excitations of the lattice in multicomponent magnets produce no discernible change in magnetic moment in the absence of the laser pulse, i.e., the effect that we describe is profoundly nonadiabatic.

RESULTS

Electron phonon coupling

To manipulate spin dynamics via selected phonon modes, as a first step, we examine the phonon spectra and electron-phonon coupling (EPC), shown in Fig. 1A for FePt. The EPC strength is shown as the width of the phonon modes in this figure. Evidently, the EPC is strongest for the optical phonon modes at the X-point (*25*), and an analysis of the phonon modes indicates that the two strongly coupled modes are the pure in-plane Fe mode and the pure in-plane Pt mode (see Fig. 1D) with a period of ~191 fs. $L1_0$ structure can be viewed as planes of Pt and Fe atoms (see Fig. 1B), and in-plane refers to the direction parallel to these planes (this does not refer to the coupling of the mode to the external field). With this information in hand, we now study the dynamics of the pump laser–excited spin system in the presence of such modes. In doing so, we have in mind a double-pump setup where these phonons are preexcited,

[1]Max-Born-Institut für Nichtlineare Optik und Kurzzeitspektroskopie, Max-Born-Strasse 2A, 12489 Berlin, Germany. [2]Max-Planck-Institut für Mikrostrukturphysik, Weinberg 2, D-06120 Halle, Germany.
*Corresponding author. Email: sharma@mbi-berlin.de

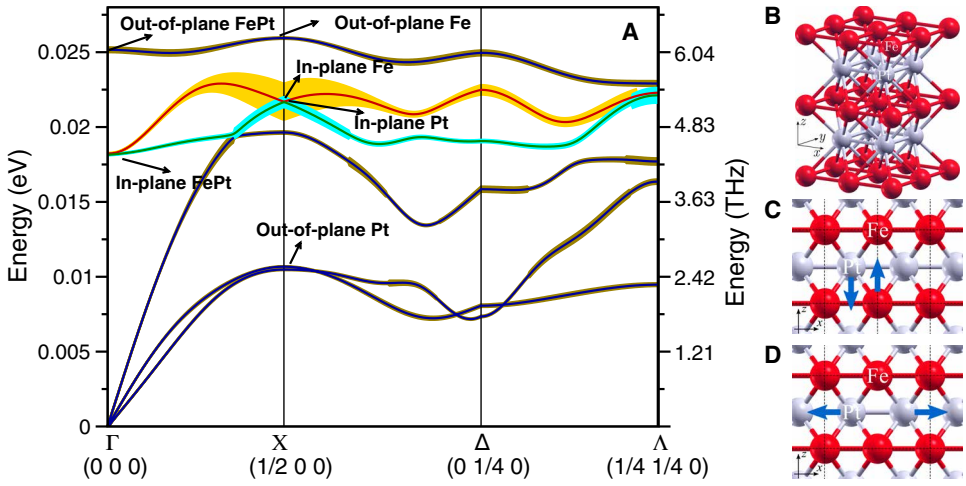

Fig. 1. Phonon spectra (along Γ–X–Δ–Λ direction) for FePt with EPC strength indicated by the width of the spectral line. (**A**) The phonon energies are given in electron volts on the left with the corresponding values shown in terahertz on the right. As can be seen (width of the orange curve), the EPC is strongest at the X-point (for details of the nature of these modes, see the legend), (**B**) the $L1_0$ structure (two unit cells in the *x* direction) with Fe atoms as red and Pt atoms as gray; (**C**) out-of-plane Fe-Pt mode at Γ-point, which has a period of 165 fs; (**D**) in-plane Pt mode at X-point, which has a period of 191 fs.

following which an optical laser pump pulse is used to manipulate spins in the presence of the excited phonon modes.

Femto-phono-magnetism

In Fig. 2 (A and B), the results are shown for the spin dynamics of FePt under the influence of a pump pulse and in the presence of the two strongly coupled X-point phonon modes of time period 191 fs with the phonon amplitude set to 1.1 pm (0.275% of the lattice constant). The laser pulse is shown in gray and has a central frequency of 1.55 eV (800 nm or 374.8 THz), incident fluence of 9 mJ/cm^2 (i.e., amplitude, 2×10^{12} W/cm), duration (i.e., full width at half maximum) of 13 fs, and is polarized in the plane of the phonon mode; this pulse will be used in all calculations unless stated. The phase difference between the phonon and laser pulse maxima represents an important parameter that we will subsequently discuss in depth; here, we set this difference to 20 fs, which, as can be seen from the atomic displacement curve plotted in Fig. 2 (A and B), ensures that the system is laser excited close to the maxima of the phononic disturbance of the lattice. In Fig. 2, we display the atom-resolved normalized moments both with full nuclear dynamics (i.e., including both the effect of the preexcited phonon and the forces acting on the nuclei due to the transfer of momentum from the electronic system) and in the absence of nuclear dynamics.

For these modes, the two Pt (or Fe) atoms move in-plane (see Fig. 1D) and in mutually opposite directions. Unexpectedly, we see that the in-plane Pt mode has a significant effect on the spin dynamics with demagnetization of the Fe atom increasing by 0.5 bohr magneton (μ_B) per Fe atom (20% of the ground-state moment), an effect that occurs in less than 40 fs after the pump pulse (see Fig. 2). At early times (<25 fs), the moment on the Fe lattice decreases with a corresponding increase in the moment of the Pt sublattice, a signature of OISTR (see fig. S2) (*4*). The induced moment on the Pt site subsequently decreases and also shows a profoundly different spin dynamics in the presence and absence of nuclear dynamics. These results highlight the fact that the nuclear dynamics, long assumed to be important only as an energy and momentum reservoir, can,

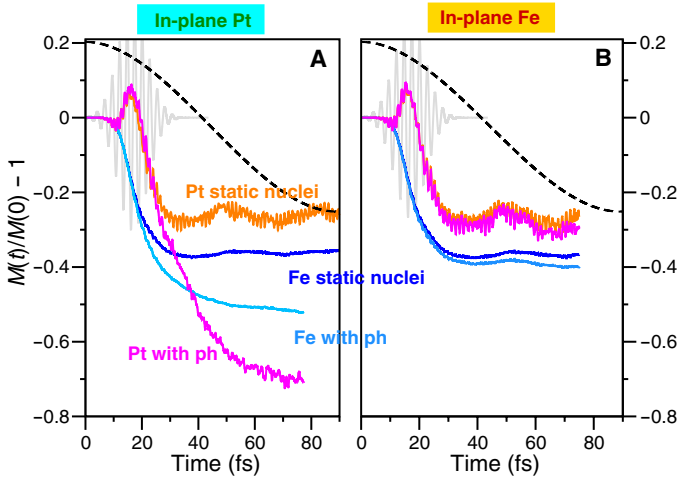

Fig. 2. Normalized atom-resolved spin moment as a function of time (in femtoseconds) in laser-pumped FePt, with the vector potential of the laser pulse shown in gray. Spin dynamics calculations are performed both for full nuclear dynamics (i.e., including both preexcitation of the phonon and forces generated on the nuclei by momentum transfer from the excited electron system) and in the absence of nuclear dynamics. Displacement of atoms during the phonon modes is shown with black dashed lines. Results are shown for the two most strongly coupled phonon modes at the X-point: (**A**) the in-plane Pt mode (see Fig. 1D) and (**B**) the in-plane Fe mode.

when selectively preexcited, decisively influence ultrafast demagnetization, allowing for faster spin manipulation times. We should stress that the nuclear dynamics includes forces arising from (i) the preexcited phonon and (ii) from the transfer of momentum from the excited electronic system (this includes the effect of the optical pump pulse on the lattice). The forces acting on the nuclei from the latter effect represent less than 5% of the total force, and their inclusion does not significantly change the influence of the lattice on the spin dynamics, which is dominated by the preexcited phonon in these early times (see fig. S2).

Although the in-plane Fe mode has a very strong EPC, the effect of this mode on the spin dynamics is insignificant at early times. This indicates that large EPC, while useful as a guide, does not necessarily imply large spin-phonon coupling. It should thus be stressed that an approach based on calculating EPC and exchange constants from equilibrium cannot provide a reliable guide for calculating spin and nuclear dynamics at early times.

For the phonon amplitude discussed thus far, 1.1 pm (0.275% of the lattice constant), the corresponding adiabatic nuclear displacements result in no significant change in the spin magnetic moment; if the nuclei are displaced to the maximum amplitude of the phonon and the ground-state moment determined, then it changes by merely 0.009 μ_B per Fe atom and 0.0008 μ_B per Pt atom as compared to the moment without any displacement. We further find that the dynamics of the spin moment due to the pump pulse, if we fix the nuclei to be displaced at the maximum position, are also the same as without any displacement. The effect of nuclear degrees of freedom on spins in this case of multicomponent magnet is thus profoundly nonadiabatic; displacement of the nuclei that results in essentially no change to the moment when performed statically on the ground state has a profound impact when performed dynamically in combination with laser excitation of the electron system. Last, when several modes are excited together, the mode that strongly influences the magnetization dominates the physics of phonomagnetism; we demonstrate this by exciting in-plane Pt and out-of-plane Fe modes simultaneously and noting that in-plane Pt mode dominates, as can be seen by comparison of (A) and (B) of Fig. 3.

IR active phonons

Selective excitation of finite momentum X-point phonons requires considerable effort (*30*–*32*), with the experimentally easily accessible phonon excitations being the IR active phonon modes at Γ-point. While the equilibrium EPC is negligible for these phonons, a key finding thus far is that, by itself, this cannot serve as a means to predict the strength of the dynamic coupling between preexcited phonons and demagnetization. We thus now examine how changing both the wave vector from X to Γ and phonon amplitude affects the spin dynamics.

In Fig. 4, we present femto-phono-magnetism at the Γ-point, with the impact on demagnetization of the IR active (6.04-THz) out-of-plane Fe-Pt mode (in which the Fe and Pt planes oscillate parallel to the spin quantization axis and in opposite directions to each other with a duration of 165 fs; see Fig. 1C shown for amplitudes of 1.1 and 2.4 pm). Note that this latter amplitude (0.6% of the lattice constant) produces, upon adiabatic displacement of the nuclei, a negligible change in ground-state moment (of 0.0095 μ_B per Fe atom).

Despite the much reduced EPC at the Γ-point, a new feature of femto-phono-magnetism emerges with the IR active (6.04-THz) out-of-plane Fe-Pt mode now significantly affecting the magnetization dynamics, with an extra 30% per Fe atom demagnetization at 85 fs for the amplitude of 2.4 pm. Reducing the pump laser pulse fluence to 2 mJ/cm^2, this enhancement of demagnetization increases to 40% (see fig. S3). For comparison, we show the X-point phonon mode also at amplitudes of 1.1 and 2.4 pm (see Fig. 4B), which shows a small difference in the amount of demagnetization going from 1.1 to 2.4 pm. That the IR active mode can also be used to strongly manipulate spins makes the present results highly significant and directly accessible by experiments.

Spin current

To further probe the reasons behind this enhanced demagnetization due to nonadiabatic coupled spin-nuclear dynamics, we now look at the transient spin-dependent charge. We consider the case of the Γ-point out-of-plane Fe-Pt mode with an amplitude of 2.4 pm and a pump laser pulse with a central frequency of 1.55 eV, a duration of 13 fs, and an incident fluence of 9 mJ/cm^2, with the difference between phonon and laser pulse maxima again being 20 fs, stressing that we choose this merely as a representative case; similar physics

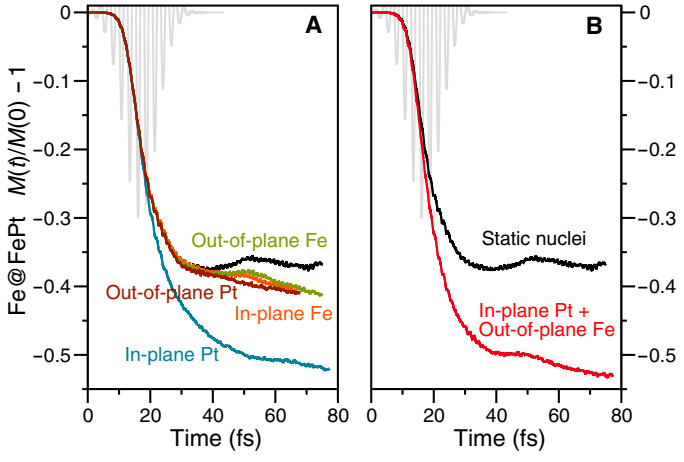

Fig. 3. Normalized Fe atom–projected spin moment as a function of time (in femtoseconds) in laser-pumped FePt. The same pump pulse as in Fig. 2 is used (the vector potential is shown in gray). The magnetic moments are shown both with full nuclear dynamics (i.e., including both preexcitation of the phonon and forces generated on the nuclei by momentum transfer from the excited electron system) and in the absence of nuclear dynamics. Results are shown for (**A**) different X-point phonon modes (see the legend and Fig. 1A for mode details) and (**B**) when two X-point modes are excited together. For a direct comparison, the amplitude of all the modes is kept constant at 1.1 pm (0.275% of the lattice constant).

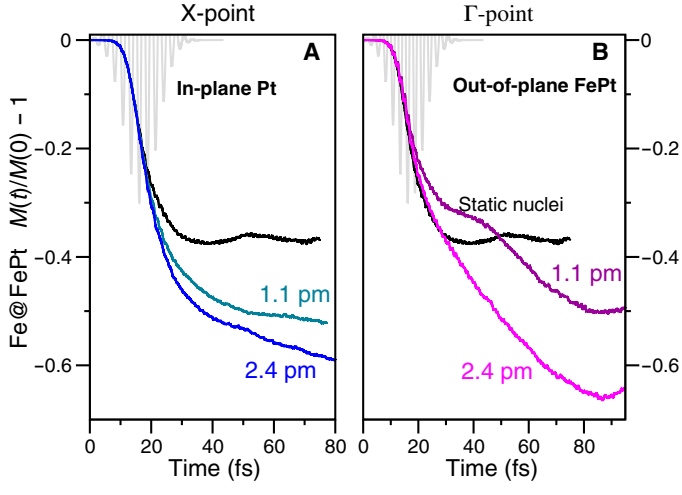

Fig. 4. Normalized Fe atom–projected spin moment as a function of time (in femtoseconds) in laser-pumped FePt. The pump pulse vector potential is shown in gray. The moment is calculated in the presence of phonon modes and in the absence of any nuclear motion. Results are shown for phonon modes with two different amplitudes: (**A**) the in-plane X-point Pt mode and (**B**) out-of-plane Γ-point Fe-Pt mode.

is found to underpin all cases where the preexcited phonon substantially affects the spin dynamics.

In Fig. 5, the difference between transient charge with and without inclusion of nuclear dynamics is plotted and shown projected onto spin and atom type. As can be seen, in the coupled nuclear and spin dynamics, the main role is played by minority charge with the presence of a preexcited phonon shown to result in a substantially increased flow of minority spin current from Fe to Pt. This, in turn, dynamically increases the number of available Fe minority states, leading to increased majority-to-minority spin flips on the Fe site and a large demagnetization of both Fe and Pt sublattices. This flow of minority spin current from Fe to Pt atoms is due to a large number of available Pt minority states (see the density of state for FePt in fig. S1). It has been recently shown that such currents can be very important for terahertz generation (*33*), which is a radiative effect and is of crucial importance at later times. In the future, it would be interesting to study light emission caused by phonomagnetism.

The generation of enhanced current (in particular, in minority spin channel) due to phonons is reasonable in that the nuclear motion drags charge (due to the gradient term in Eq. 2), constituting a current that, in the absence of the pump pulse, would simply move charge back and forth. However, in the presence of the pump pulse, the current (and magnetization) does not oscillate with phonon mode but instead results in a pronounced intersite charge transfer. This current is dominated in the minority spin channel due to available empty states above the Fermi level.

A further effect of nuclear-spin coupling that we find is a localization of high-energy delocalized electrons, with delocalized charge decreasing in both spin channels (see Fig. 5C). This physics has recently also been seen in graphite where high energy charge (6 to 8 eV above the Fermi level) is localized and stabilized because of phonons (*34*). Thus, the highlight of these results is that the minority spin current between sublattices controls the physics in the case of nonadiabatic spin-phonon coupling.

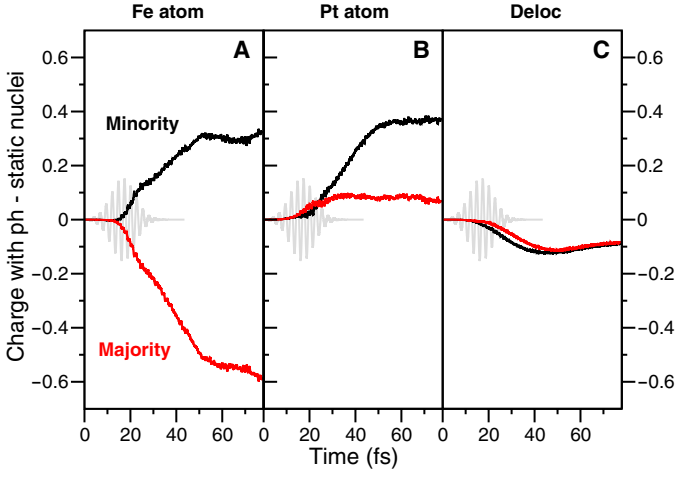

Fig. 5. Difference in atom- and spin-resolved charge calculated with and without phonons for laser-pumped FePt. The calculations with phonons were performed in the presence of the in-plane X-point Pt mode. The same pump pulse (vector potential shown in gray in each panel) is used as in Fig. 2. Results are shown for (**A**) the Fe atom, (**B**) the Pt atom, and (**C**) delocalized charge in highly excited states that cannot be assigned to either atom.

Phase between phonon mode and pump pulse

To examine the effect of the timing of the pump pulse with respect to the nuclear displacement, we examine the effect of various pump pulse delays for the case of the Γ-point out-of-plane Fe-Pt phonon mode with an amplitude of 2.4 pm, i.e., 0.6% of the lattice constant (see Fig. 6). The pump pulse has a central frequency of 1.55 eV, a duration of 13 fs (7.8% of the phonon cycle), and the incident fluence of 2 mJ/cm^2. For this pulse, we see similar spin dynamics (see Fig. 6, F, G, and I) for all pump pulse delays, except for the case in which the pump pulse maximum coincides with the zero displacement of the nuclei (see Fig. 6H), where the demagnetization amplitude is, in comparison, not strongly affected by the presence of the phonon mode. This highlights the fact that the phonons couple strongly to the excited electrons. Experimentally, it would be difficult to control this phase of the pump pulse with respect to the nuclear displacement, so we now demonstrate that this problem can be circumvented by the use of a longer pump pulse of duration of 25 fs (15% of the phonon cycle). For these simulations, the incident fluence of the pump pulse is kept fixed, and so, to increase the duration, the amplitude of the pump pulse is thus correspondingly reduced. These results are shown in Fig. 6 (E and J) where the strong effect of phonons on the demagnetization dynamics is restored despite the pulse maxima coinciding with the node of the phonon displacement.

DISCUSSION

We demonstrate that for multicomponent magnet, (i) nuclear degrees of freedom do not merely act as energy sink for pumped spins, but they can also be used to enhance spin-dynamical effects at femtosecond time scales, (ii) that this enhancement occurs through profoundly nonadiabatic spin-phonon coupling, and (iii) that the microscopic mechanism underpinning this effect of femto-phonomagnetism is a substantial increase in the minority spin current flow between sublattices with concomitant increase in spin-orbit coupling (SOC) spin flips into empty minority states, in turn resulting in enhanced demagnetization. We have examined both finite momentum

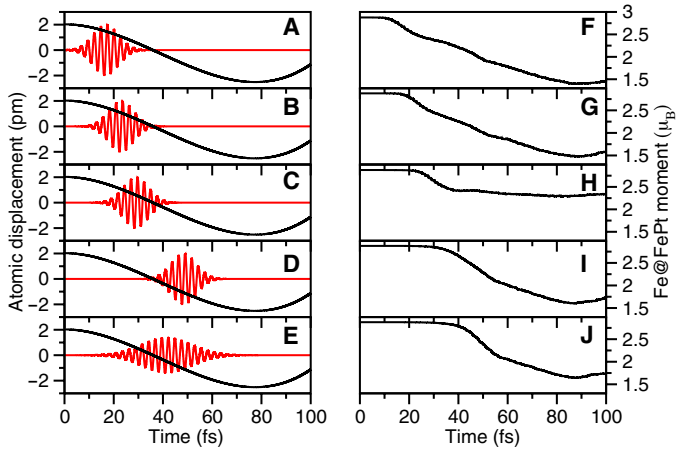

Fig. 6. System is pumped with a laser pulse at different times during the phonon mode. The displacement of atoms during the phonon mode (solid black line) and the vector potential of the pump laser pulse (red) are shown in (**A**) to (**E**). The corresponding magnetic moment (in bohr magneton) as a function of time (in femtoseconds) for the Fe atoms in FePt is shown in (**F**) to (**J**).

X-point phonons and IR active Γ-point phonons. We find that specific phonon modes dominate the spin dynamics, such that mixing with nondominant modes has little effect on the overall demagnetization.

These results open a route toward spin manipulation by small-amplitude coherent phonons in femtosecond spin dynamics in multicomponent metallic magnets. The mechanism of intersite minority current flow suggests that such multicomponent magnetic materials will present a rich field for spin manipulation via nuclear degrees of freedom, with similar physics expected to be found at interfaces between magnetic materials or a magnetic and nonmagnetic material, in which interface currents will be controlled by interface phonon modes. In the future, it would also be interesting to explore the effects of such currents on light emission. Our results thus suggest a powerful new route to controlling magnetic order at femtosecond time scales with the nuclear and electron systems both now viewed as key degrees of freedom for the ultrafast manipulation of the spin degree of freedom.

MATERIALS AND METHODS

To study the dynamics of the spin and charge, we have used fully ab initio state-of-the-art TDDFT (*22*). For the intense laser pulses, we consider here that it is necessary to accurately describe bands within a wide energy range of the Fermi level. Low-energy models in combination with a dynamical mean field theory treatment of correlation (*35*), essential for treating the low-energy sector of strongly correlated insulators under weak laser excitation, are thus not appropriate for the strong laser pulse excitation of weakly correlated metallic systems that we consider here.

TDDFT rigorously maps the computationally intractable problem of interacting electrons to the Kohn-Sham (KS) system of noninteracting Fermions in a fictitious potential, which can be solved by modern computing clusters. The time-dependent KS equation is

$$i\frac{\partial \psi_{j\boldsymbol{k}}(\mathbf{r},t)}{\partial t} = \left[\frac{1}{2}\left(-i\nabla+\frac{1}{c}\mathbf{A}_{\mathrm{ext}}(t)\right)^2+v_s(\mathbf{r},t)+\frac{1}{2c}\sigma\cdot\mathbf{B}_s(\mathbf{r},t)+\frac{1}{4c^2}\sigma\cdot(\nabla v_s(\mathbf{r},t)\times -i\nabla)\right]\psi_{j\boldsymbol{k}}(\mathbf{r},t) \quad (1)$$

where $\mathbf{A}_{\mathrm{ext}}(t)$ is a vector potential representing the applied laser field. It is assumed that the wavelength of the applied laser is much greater than the size of a unit cell, and the dipole approximation can be used, i.e., the spatial dependence of the vector potential is disregarded. The KS fictitious potential $v_s(\mathbf{r}, t) = v_{\mathrm{ext}}(\mathbf{r}, t) + v_{\mathrm{H}}(\mathbf{r}, t) + v_{\mathrm{xc}}(\mathbf{r}, t)$ is decomposed into the external potential v_{ext}, the classical electrostatic Hartree potential v_{H}, and the exchange correlation (XC) potential v_{xc}. Similarly, the KS magnetic field is written as $\mathbf{B}_s(\mathbf{r}, t) = \mathbf{B}_{\mathrm{ext}}(t) + \mathbf{B}_{\mathrm{xc}}(\mathbf{r}, t)$, where $\mathbf{B}_{\mathrm{ext}}(t)$ is an external magnetic field, and $\mathbf{B}_{\mathrm{xc}}(\mathbf{r}, t)$ is the exchange correlation (XC) magnetic field. σ are the Pauli matrices. The final term of Eq. 1 is the spin-orbit coupling term.

The back-reaction of the nuclear dynamics on the electronic system is approximated with

$$v_s(\mathbf{r},t) \rightarrow v_s(\mathbf{r},t) - \sum_{p\alpha}\frac{\partial v_{\mathrm{cl}}(\mathbf{r})}{\partial u_\alpha^p}\delta u_\alpha^p(t) \quad (2)$$

where p labels a nucleus and α is the direction. v_{cl} is the Coulomb potential from the nucleus and the core density of electrons. $\delta u_\alpha^p(t)$ is the displacement of the nucleus away from equilibrium and is calculated from the atomic forces (*36*). There are two contributions to the forces generated on the nuclei that lead to nuclear dynamics: (i) motion of electronic charge due to the pump laser pulse (*37*) [this is responsible for the transfer of angular momentum from the spin system to the lattice (*38*) and the effect of the laser pulse on the lattice] and (ii) the forces due to nuclei being out of equilibrium caused by excitation of phonon modes. These forces then cause the nuclei to move according to the classical equations of motion. These moving nuclei themselves cause a back-reaction on the electronic system as described above. This back-reaction ultimately also affects the forces on the nuclei again; however, such higher-order effects are neglected in the present work. This formalism is exact in the small displacement limit and is suited to methods where the basis itself depends on the position of the nucleus, as in the present case, where a state-of-the-art highly accurate full-potential linearized augmented plane wave basis (*39*) is used.

Computational parameters

All calculations are performed for $L1_0$ structure (see Fig. 1B) of FePt with lattice (*40*) parameter $a = 3.88$ Å and $c = 3.73$ Å. A **k**-point set of $12 \times 12 \times 8$ was used for real-time TDDFT calculations. The phonon spectra and calculation of EPC require a finer **k**-point grid, and we have used a grid of $24 \times 24 \times 20$. All states up to 50 eV above the Fermi energy were included in our calculations. For time propagation, we have used a time step of 2.42 as; more details of the time propagation algorithm can be found in (*41*). A smearing width of 0.027 eV was used for the ground state and for time propagation. In all calculations, we use the adiabatic local density functional, which has been shown to be highly accurate in treating very early time spin dynamics (*4*–*6*, *23*, *24*). All calculations are performed using the Elk code (*42*).

Phonon modes

The X-point phonons are excited by making a $2 \times 1 \times 1$ supercell. The period of these in-plane Fe and Pt X-point phonons is 191 fs. The Γ-point optical out-of-plane FePt phonon can be described within a single unit cell and has a time period of 165 fs.

SUPPLEMENTARY MATERIALS

Supplementary material for this article is available at https://science.org/doi/10.1126/sciadv.abq2021

REFERENCES AND NOTES

1. D. N. Basov, R. D. Averitt, D. Hsieh, Towards properties on demand in quantum materials. *Nat. Mater.* **16**, 1077–1088 (2017).
2. A. Kirilyuk, A. V. Kimel, T. Rasing, Ultrafast optical manipulation of magnetic order. *Rev. Mod. Phys.* **82**, 2731–2784 (2010).
3. T. Itoh, Derivation of nonrelativistic Hamiltonian for electrons from quantum electrodynamics. *Rev. Mod. Phys.* **37**, 159–165 (1965).
4. J. K. Dewhurst, P. Elliott, S. Shallcross, E. K. U. Gross, S. Sharma, Laser-induced intersite spin transfer. *Nano Lett.* **18**, 1842–1848 (2018).
5. F. Siegrist, J. A. Gessner, M. Ossiander, C. Denker, Y. P. Chang, M. C. Schröder, A. Guggenmos, Y. Cui, J. Walowski, U. Martens, J. K. Dewhurst, U. Kleineberg, M. Münzenberg, S. Sharma, M. Schultze, Light-wave dynamic control of magnetism. *Nature* **571**, 240–244 (2019).
6. K. Krieger, J. K. Dewhurst, P. Elliott, S. Sharma, E. K. U. Gross, Laser-induced demagnetization at ultrashort time scales: Predictions of TDDFT. *J. Chem. Theory Comput.* **11**, 4870–4874 (2015).
7. G. P. Zhang, W. Hübner, Laser-induced ultrafast demagnetization in ferromagnetic metals. *Phys. Rev. Lett.* **85**, 3025–3028 (2000).
8. J. K. Dewhurst, S. Shallcross, E. K. U. Gross, S. Sharma, Substrate-controlled ultrafast spin injection and demagnetization. *Phys. Rev. Applied* **10**, 044065 (2018).
9. K. Jhuria, J. Hohlfeld, A. Pattabi, E. Martin, A. Y. Arriola Córdova, X. Shi, R. Lo Conte, S. Petit-Watelot, J. C. Rojas-Sanchez, G. Malinowski, S. Mangin, A. Lemaître, M. Hehn,

J. Bokor, R. B. Wilson, J. Gorchon, Spin-orbit torque switching of a ferromagnet with picosecond electrical pulses. *Nat. Electron.* **3**, 680–686 (2020).
10. R. Mikhaylovskiy, E. Hendry, A. Secchi, J. H. Mentink, M. Eckstein, A. Wu, R. V. Pisarev, V. V. Kruglyak, M. I. Katsnelson, T. Rasing, A. V. Kimel, Ultrafast optical modification of exchange interactions in iron oxides. *Nat. Commun.* **6**, 8190 (2015).
11. C. Dornes, Y. Acremann, M. Savoini, M. Kubli, M. J. Neugebauer, E. Abreu, L. Huber, G. Lantz, C. A. F. Vaz, H. Lemke, E. M. Bothschafter, M. Porer, V. Esposito, L. Rettig, M. Buzzi, A. Alberca, Y. W. Windsor, P. Beaud, U. Staub, D. Zhu, S. Song, J. M. Glownia, S. L. Johnson, The ultrafast Einstein-de Haas effect. *Nature* **565**, 209–212 (2019).
12. S. R. Tauchert, M. Volkov, D. Ehberger, D. Kazenwadel, M. Evers, H. Lange, A. Donges, A. Book, W. Kreuzpaintner, U. Nowak, P. Baum, Polarized phonons carry angular momentum in ultrafast demagnetization. *Nature* **602**, 73–77 (2022).
13. M. Rini, R. Tobey, N. Dean, J. Itatani, Y. Tomioka, Y. Tokura, R. W. Schoenlein, A. Cavalleri, Control of the electronic phase of a manganite by mode-selective vibrational excitation. *Nature* **449**, 72–74 (2007).
14. R. Mankowsky, A. von Hoegen, M. Först, A. Cavalleri, Ultrafast reversal of the ferroelectric polarization. *Phys. Rev. Lett.* **118**, 197601 (2017).
15. T. F. Nova, A. S. Disa, M. Fechner, A. Cavalleri, Metastable ferroelectricity in optically strained SrTiO3. *Science* **364**, 1075–1079 (2019).
16. M. Deb, E. Popova, S. P. Zeuschner, M. Hehn, N. Keller, S. Mangin, G. Malinowski, M. Bargheer, Generation of spin waves via spin-phonon interaction in a buried dielectric thin film. *Phys. Rev. B* **103**, 024411 (2021).
17. E. A. Mashkovich, K. A. Grishunin, R. M. Dubrovin, A. K. Zvezdin, R. V. Pisarev, A. V. Kimel, Terahertz light-driven coupling of antiferromagnetic spins to lattice. *Science* **374**, 1608–1611 (2021).
18. Y. Zhang, X. Shi, W. You, Z. Tao, Y. Zhong, F. Cheenicode Kabeer, P. Maldonado, P. M. Oppeneer, M. Bauer, K. Rossnagel, H. Kapteyn, M. Murnane, Coherent modulation of the electron temperature and electron-phonon couplings in a 2D material. *Proc. Natl. Acad. Sci.* **117**, 8788–8793 (2020).
19. D. Shin, H. Hübener, U. de Giovannini, H. Jin, A. Rubio, N. Park, Phonon-driven spin-floquet magneto-valleytronics in MoS2. *Nat. Commun.* **9**, 638 (2018).
20. D. Afanasiev, J. R. Hortensius, B. A. Ivanov, A. Sasani, E. Bousquet, Y. M. Blanter, R. V. Mikhaylovskiy, A. V. Kimel, A. D. Caviglia, Ultrafast control of magnetic interactions via light-driven phonons. *Nat. Mater.* **20**, 607–611 (2021).
21. D. M. Juraschek, P. Narang, N. A. Spaldin, Phono-magnetic analogs to opto-magnetic effects. *Phys. Rev. Res.* **2**, 043035 (2020).
22. E. Runge, E. K. U. Gross, Density-functional theory for time-dependent systems. *Phys. Rev. Lett.* **52**, 997–1000 (1984).
23. M. Hofherr, S. Häuser, J. K. Dewhurst, P. Tengdin, S. Sakshath, H. T. Nembach, S. T. Weber, J. M. Shaw, T. J. Silva, H. C. Kapteyn, M. Cinchetti, B. Rethfeld, M. M. Murnane, D. Steil, B. Stadtmüller, S. Sharma, M. Aeschlimann, S. Mathias, Ultrafast optically induced spin transfer in ferromagnetic alloys. *Sci. Adv.* **6**, eaay8717 (2020).
24. F. Willems, C. von Korff Schmising, C. Strüber, D. Schick, D. W. Engel, J. K. Dewhurst, P. Elliott, S. Sharma, S. Eisebitt, Optical inter-site spin transfer probed by energy and spin-resolved transient absorption spectroscopy. *Nat. Commun.* **11**, 871 (2020).
25. P. Maldonado, K. Carva, M. Flammer, P. M. Oppeneer, Theory of out-of-equilibrium ultrafast relaxation dynamics in metals. *Phys. Rev. B* **96**, 174439 (2017).
26. D. Weller, O. Mosendz, G. Parker, S. Pisana, T. S. Santos, $L1_0$ FePtX–Y media for heat-assisted magnetic recording. *Phys. Status Solid A* **210**, 1245–1260 (2013).
27. A. Giri, S. H. Wee, S. Jain, O. Hellwig, P. E. Hopkins, Influence of chemical ordering on the thermal conductivity and electronic relaxation in FePt thin films in heat assisted magnetic recording applications. *Sci. Rep.* **6**, 32077 (2016).
28. D. Turenne, A. Yaroslavtsev, X. Wang, V. Unikandanuni, I. Vaskivskyi, M. Schneider, E. Jal, R. Carley, G. Mercurio, R. Gort, N. Agarwal, B. Van Kuiken, L. Mercadier, J. Schlappa, L. L. Guyader, N. Gerasimova, M. Teichmann, D. Lomidze, A. Castoldi, D. Potorochin, D. Mukkattukavil, J. Brock, N. Z. Hagström, A. H. Reid, X. Shen, X. J. Wang, P. Maldonado, Y. Kvashnin, K. Carva, J. Wang, Y. K. Takahashi, E. E. Fullerton, S. Eisebitt, P. M. Oppeneer, S. Molodtsov, A. Scherz, S. Bonetti, E. Iacocca, H. A. Dürr, Nonequilibrium sub-10 nm spin-wave soliton formation in FePt nanoparticles. *Sci. Advs.* **8**, eabn0523 (2022).
29. C.-H. Lambert, S. Mangin, B. S. D. C. S. Varaprasad, Y. K. Takahashi, M. Hehn, M. Cinchetti, G. Malinowski, K. Hono, Y. Fainman, M. Aeschlimann, E. E. Fullerton, All-optical control of ferromagnetic thin films and nanostructures. *Science* **345**, 1337–1340 (2014).
30. A. T. Tarekegne, B. Zhou, K. Kaltenecker, K. Iwaszczuk, S. Clark, P. U. Jepsen, Terahertz time-domain spectroscopy of zone-folded acoustic phonons in 4h and 6h silicon carbide. *Opt. Express* **27**, 3618–3628 (2019).
31. R. Samnakay, D. Wickramaratne, T. R. Pope, R. K. Lake, T. T. Salguero, A. A. Balandin, Zone-folded phonons and the commensurate-incommensurate charge-density-wave transition in 1T-TaSe2 thin films. *Nano Lett.* **5**, 2965–2973 (2015).
32. A. S. Disa, T. S. Nova, A. Cavalleri, Engineering crystal structures with light. *Nat. Phys.* **17**, 1087–1092 (2021).
33. M. Runge, T. Kang, K. Biermann, K. Reimann, M. Woerner, T. Elsaesser, Mono-cycle terahertz pulses from intersubband shift currents in asymmetric semiconductor quantum wells. *Optica* **8**, 1638 (2021).
34. T. P. H. Sidiropoulos, N. di Palo, D. E. Rivas, S. Severino, M. Reduzzi, B. Nandy, B. Bauerhenne, S. Krylow, T. Vasileiadis, T. Danz, P. Elliott, S. Sharma, K. Dewhurst, C. Ropers, Y. Joly, M. E. Garcia, M. Wolf, R. Ernstorfer, J. Biegert, Probing the energy conversion pathways between light, carriers, and lattice in real time with attosecond core-level spectroscopy. *Phys. Rev. X* **11**, 041060 (2021).
35. D. Afanasiev, A. Gatilova, D. J. Groenendijk, B. A. Ivanov, M. Gibert, S. Gariglio, J. Mentink, J. Li, N. Dasari, M. Eckstein, T. Rasing, A. D. Caviglia, A. V. Kimel, Ultrafast spin dynamics in photodoped spin-orbit mott insulator Sr_2IrO_4. *Phys. Rev. X* **9**, 021020 (2019).
36. R. Yu, D. Singh, H. Krakauer, All-electron and pseudopotential force calculations using the linearized-augmented-plane-wave method. *Phys. Rev. B* **43**, 6411–6422 (1991).
37. Y. Shinohara, K. Yabana, Y. Kawashita, J. I. Iwata, T. Otobe, G. F. Bertsch, Coherent phonon generation in time-dependent density functional theory. *Phys. Rev. B* **82**, 155110 (2010).
38. J. K. Dewhurst, S. Shallcross, P. Elliott, S. Eisebitt, C. K. Schmising, S. Sharma, Angular momentum redistribution in laser-induced demagnetization. *Phys. Rev. B* **104**, 054438 (2021).
39. D. J. Singh, *Planewaves Pseudopotentials and the LAPW Method* (Kluwer Academic Publishers, 1994).
40. A. Alsaad, A. Ahmad, T. S. Obeidat, Structural, electronic and magnetic properties of the ordered binary FePt, MnPt, and $CrPt_3$ alloys. *Heliyon* **6**, 203545 (2020).
41. J. K. Dewhurst, K. Krieger, S. Sharma, E. K. U. Gross, An efficient algorithm for time propagation as applied to linearized augmented plane wave method. *Comput. Phys. Commun.* **209**, 92–95 (2016).
42. J. K. Dewhurst, S. Sharma, *et al.*, elk.sourceforge.net (14 January 2018).

Acknowledgments: We acknowledge the North-German Supercomputing Alliance (HLRN) for providing HPC resources that have contributed to the research results reported in this paper. **Funding:** S.Shar. and J.K.D. would like to thank the DFG for funding through project-ID 328545488 TRR227 (projects A04). S.Shal. would like to thank the DFG for funding through SPP 1840 QUTIF grant no. SH 498/3-1, while P.E. thanks the DFG for funding through project 2059421. This work was supported by the DFG. **Author contributions:** J.K.D. designed the algorithm and wrote the code. S.Shar. designed the project and performed the calculations. S.Shal. and P.E. contributed to the analysis. All authors contributed to the writing of the manuscript. **Competing interests:** The authors declare that they have no competing interests. **Data and materials availability:** All data needed to evaluate the conclusions in the paper are present in the paper and/or the Supplementary Materials. The code used in the manuscript is accessible at https://elk.sourceforge.io/.

Submitted 24 March 2022
Accepted 28 July 2022
Published 14 September 2022
10.1126/sciadv.abq2021